10.3.2 In vivo measurements

10.3.2.1 Introduction

Internal exposures due to incorporation of radioactive materials may be detected both by *in vivo* and *in vitro* measurement: the *in vivo* measurement involves the measurement by detectors external to the body, thus mainly radionuclides emitting γ or X-rays can be detected by this way. The *in vitro* method is based on the measurement of the activity excreted with the urine, faeces and exhaled air and thus can be applied in principle for any material. In many cases the *in vitro* method is more sensitive but the interpretation of the results is in general more difficult because of the lack of information with respect to the individual metabolic behaviour of the incorporated materials. The *in vivo* method is not as sensitive as the *in vitro* method but the evaluation of the results is more easy because not that much information is needed for the assessment of dose from body or organ activity data. So the *in vivo* measurement is considered to be the best method for the detection of γ emitting radionuclides i.e. most of the fission and activation products and few actinides such as ^{235}U or transuranium radionuclides such as ^{241}Am, whereas the *in vitro* method is applied for the detection of all other radionuclides where the in *vivo* method is not sensitive enough. In few cases the *in vivo* technique can be applied also for α-emitters with γ emitting daughters, such as ^{226}Ra or ^{238}U.

The first *in vivo* measurements of Radium have been carried out in 1927 by Blumgart and Weiss using ionisation chambers for blood flow studies [27Blu]. The lower detection limit of those measurements was reported to vary in the range from 5 to 100 μg (0.18 to 3.7 MBq) ^{226}Ra, assuming radiological equilibrium between ^{226}Ra and its γ-emitting daughter products [29Sch]. In 1931 Schlundt took into account the geometry and the self-absorption of the body by inserting sealed radon sources in a phantom, thus providing the first calibration standard for *in vivo* measurements [31Sch]. In those years three lethal cases of radium poisoning were established in the radium manufacturing industry in Germany, this enforcing the further development of detection procedures at the Max-Planck Institute for Biophysics in Frankfurt, Germany. So in 1938 the "Untersuchungsstelle für die physikalische Diagnostik der Radium-vergiftungen" was founded at the Kaiser-Wilhelm-Institut for Biophysics in Frankfurt. At the same time researchers in the United States applied high sensitive Geiger-Müller tubes also and the lower detection limit was reported to be 1 μg (37 kBq) ^{226}Ra [37Eva]. Few years later Rajewsky and Dreblow performed first partial body measurements using a so-called gamma-ray stethoscope which enabled the diagnosing physician to contact directly the individual parts of the body thus allowing for the localization of radium deposits in the body [41Raj]. About one decade later, Sievert developed a 4π - geometry whole-body counter using an arrangement of 10 long ionisation chambers surrounding the subject. For achieving a low background, the measuring device was installed into granite rocks 50 m below ground surface, this resulting in a detection limit of about 1 nCi (37 Bq) of ^{226}Ra for a measurement of 3 to 4 hours [51Sie, 57Sie]. In the fifties a lot of progress was achieved due to the development of new types of detectors such as NaI(Tl) scintillation detectors as well as liquid scintillation detectors [57And] and organic scintillation detectors [58Bir]. In 1956 the first technical conference on *in vivo* measurement was organised in Leeds in order to discuss the state of the art of measuring techniques. Since that time further improvements in the sensitivity and reliability of *in vivo* measurements have been achieved by the use of arrays of scintillation detectors and the application of anticoincidence techniques for the reduction of the detectors' background. In 1968 Laurer presented the first dual NaI(Tl)/Cs(Tl) scintillation crystal detector (phoswich) which was designed especially for low energy photon detection [68Lau]. In the late sixties semi-conductor detectors were introduced for *in vivo* measurement, starting with Lithium-drifted Germanium (Ge(Li)) detectors, which later on have been replaced by high purity Germanium (HPGe) detectors.

With improving measuring techniques, whole-body counting has become a standard method for radiation protection. Personnel working in nuclear installations or in laboratories handling radioactive materials may receive internal radioactive contamination by inhalation, ingestion or intake through wounds. Techniques of *in vivo* measurement may be employed in the monitoring and control of such contamination, either as the sole means of evaluation or in conjunction with *in vitro* measurement of activity excreted by the subject or present in the working environment.

10.3.2.2 Requirements

Techniques of *in vivo* measurement depend on the detection outside the body of photons originating from internally deposited radioactive materials. They are useful, as a means of controlling exposure to a given nuclide, if a significant deposit of that nuclide leads to a detectable signal at or near the surface of the body. In this context, a significant deposit would be one implying an intake at or exceeding some level requiring administrative action. Their feasibility in the case of a given nuclide thus depends on the yield and energy of photons emitted by the nuclide, on its pattern of deposition in the body and on the relevant limits on internal exposure. Many fission and activation products emit abundant penetrating gamma radiation, thus allowing for the assessment of intakes small in relation to annual limits, with relatively simple equipment. By contrast, long-lived α-emitters with only weak low-energy photon emissions may escape detection with the most sensitive and elaborate equipment, even when present in levels far exceeding annual limits on intake; in such instances the technique will find application only in the investigations of major acute intakes or in the monitoring of uptake following long-term chronic exposure.

In most applications, photon detectors are located at selected sites near or on the body. Usually, at least partial shielding of the detector and/or of the subject will be needed to reduce the interfering response from ambient radiation; in some cases anticoincidence techniques may be required to achieve sufficient background discrimination. Electrical signals from the detectors must be amplified and processed, leading to a gamma-ray spectrum which will most conveniently be stored in computer based systems. Procedures are necessary to separate the response attributable to a given nuclide in the body from that due to ambient radiation and to components associated with other sources of body radioactivity. The extracted response must be converted into an assessment of body or organ radioactivity through appropriate calibration procedures.

Three detection features define the requirements for *in vivo* measurement of radionuclides in the human body:

1. *Selectivity*: the capability to measure the activity of a radionuclide in the presence of other radionuclides.
2. *Sensitivity*: the response of the measuring system with respect to the level of radioactivity within the body, i.e. the capability to measure internal exposures below the limits.
3. *Accuracy*: the mean deviation of the result in terms of radioactivity from the actual radioactivity in the body or in a phantom, respectively.

Selectivity

The monitoring method has to be prepared to provide nuclide specific information, which is basic requirement for internal dose assessment. Except for circumstances where there is only one radionuclide handled by the workers to be monitored, the measurement system should provide identification of radionuclides. This means that in case of direct monitoring and also when indirect methods are applied for measuring gamma emitting radionuclides, gamma spectrometry is the method, which can meet this requirement. In this respect the semiconductor spectrometry provides better selectivity compared to scintillation spectrometry.

Sensitivity

The monitoring sensitivity should be high enough to be able to determine with proper safety an internal exposure corresponding to 1 mSv annual effective dose or 10 % of organ dose limits, respectively. To meet this requirement one has to consider the minimum detectable activity for the radionuclides to be expected, the selected monitoring frequency and a reasonable measuring time. This is illustrated by

Tables 10.12 and 10.13 which show the characteristics for some selected fission and activation products and some selected actinides, respectively. Both the energy and the yield of the predominant photon radiation of most of the fission and activation products are relative high. On the other hand the dose coefficients of these radionuclides are relatively low. So the intake corresponding to 1 mSv is rather high and thus the respective body or organ activities are high even at the end of long monitoring intervals. Contrary, the energy and the yield of the photon radiation of the actinides are typically low and the dose coefficients are high as compared to the fission and activation products.

Table 10.12. Radiological and monitoring characteristics for selected fission and activation products [83ICR, 94ICR, 04BMU]

Nuclide	Predominant photon radiation		Typical absorption type	Intake[1)] corresponding to 1 mSv eff. dose [Bq]	Routine monitoring	
	Energy [keV]	Yield [%]			Interval [d]	Required sensitivity [Bq]
^{22}Na	511 1275	180 100	F	$5 \cdot 10^5$	180	200 (Whole body)
^{57}Co	122 136	86 11	M	$2.6 \cdot 10^6$	180	20000 (Whole body)
^{60}Co	1173 1333	100 100	M	$1.4 \cdot 10^5$	180	1000 (Whole body)
^{125}I	27.2 ($K_{\alpha 2}$) 27.5 ($K_{\alpha 1}$) 31.0 ($K_{\beta 1}$) 35.5	40 74 14 6.7	F	$1.4 \cdot 10^5$	120	700 (Thyroid)
^{131}I	365	82	F	$9.1 \cdot 10^4$	14	100 (Thyroid)
^{134}Cs	569 605 796	15 98 85	F	$1 \cdot 10^5$	180	6000 (Whole body)
^{137}Cs	662	85	F	$1.5 \cdot 10^5$	180	10000 (Whole body)

1) Inhalation of aerosols with 5 µm AMAD particle size

Table 10.13. Radiological and monitoring characteristics for selected actinides [83ICR, 94ICR, 04BMU]

Nuclide	Predominant photon radiation		Typical absorption type	Intake[1)] corresponding to 1 mSv eff. dose [Bq]	Routine monitoring	
	Energy [keV]	Yield [%]			Interval [d]	Required sensitivity [Bq]
^{235}U	145 186	11 57	M	550	180	3 (Lungs)
^{239}Pu	13.6 (L_{α}) 17.1(L_{β}) 20.3 (L_{γ})	1.6 2.3 0.6	S	120	180	2 (Lungs)
^{241}Am	13.9 (L_{α}) 17.6(L_{β}) 20.3 (L_{γ}) 59.6	13.6 18.6 35.9	M	37	180	0.2 (Lungs) 0.3 (Skeleton)

1) Inhalation of aerosols with 5 µm AMAD particle size

The range of the photons in the body governs the sensitivity of *in vivo* measurement. For soft tissue the range of the 17.1 keV X-rays of ^{239}Pu is 0.89 cm, and so most of the photons emitted from an internal contamination are absorbed within the body. The range of the 1332 keV γ-rays of ^{60}Co, however, is 16.5 cm and so most of the photons emitted in the body will reach the body surface. Thus, the photon flux

at the body surface due to a ^{60}Co deposition will be at least 3 orders of magnitude higher than that due to a ^{239}Pu deposition with the same activity. Moreover, when taking into account the different dose coefficients, the photon flux due to an internal ^{60}Co exposure will be more than 6 orders of magnitude higher than that due to a ^{239}Pu exposure with the same committed effective dose, this illustrating the range of sensitivity required for *in vivo* measurements.

Accuracy

In monitoring of occupationally exposed workers for radiation protection purposes, procedures must be established to ensure that workers have exposures measured and recorded with a reasonable degree of accuracy. General requirements for the overall accuracy of the dose assessment have been recommended by the ICRP [97ICR]. Special requirements for *in vivo* measurement have been defined for example by the U.S. Department of Energy in its Laboratory Accreditation Program DOELAP [99USD]. These recommendations have been adopted by national guidelines, as for example the German Guideline for Internal Monitoring [04BMU]. The various national and international guidelines have been harmonised in the framework of the European project IDEAS [03DOE].

The accuracy of a monitoring result reflects to the quality of measurements and is usually characterized by two quantities namely by the bias and precision (repeatability).

The relative bias (B_r) is a measure of how close the assessed activity is to the actual activity in the organ(s) or in the whole body. Since the actual activity in the person is rarely known, this criterion applies to measurements on suitable phantoms that simulate the person. The relative bias statistic (B_{ri}) is defined for the purposes of performance testing of a finite number of measurements in each category of analysis by

$$B_r = \frac{1}{N}\sum_{i=1}^{N} B_{ri}$$

with

$$B_{ri} = \frac{A_i - A_{ai}}{A_{ai}} \qquad (10.3.2.1)$$

where

N is the number of test measurements in a given category ($N \geq 5$)
A_i is the value of the i^{th} measurement in the category being tested
A_{ai} is the actual quantity in the test mock-ups (phantom) for the i^{th} measurement

For service laboratories the performance requirement for the relative bias should be $0.25 \leq B_r \leq 0.50$. This requirement can only be considered if all values of A_{ai} exceed the lower limit of detection by at least factor 5.

The relative precision (S_B) describes the relative dispersion of the values of B_{ri} from their mean B_r and is defined as

$$S_B = \sqrt{\frac{\sum_{i=1}^{N}(B_{ri} - B_r)^2}{N-1}} \qquad (10.3.2.2)$$

For service laboratories the relative precision should be $S_B \leq 0.4$ for the conditions mentioned above, i.e. if all A_{ai} exceed the lower limit of detection significantly.

10.3.2.3 Principles of γ spectrometry

Photon interactions

For understanding γ spectrometry a knowledge of the basic processes by which a photon interacts with matter is essential. Three fundamental processes govern the interaction: photoelectric effect, Compton scattering and pair production. Due to these interactions the intensity $I(x)$ of the photon flux is decreasing along the pathway x according to the function

$$I(x) = I_0 \cdot e^{-\mu \cdot x} \qquad (10.3.2.3)$$

where μ is the total linear attenuation coefficient. For illustration Fig. 10.33 shows the linear attenuation coefficient of water and NaI, respectively. Water is a typical example for a low-Z material, the absorption behaviour of which is similar to soft tissue, and NaI is a typical example for a high-Z material, which is widely used for γ spectrometry. More detailed information about photon interaction can be found in Section 3.5.2.3 and elsewhere [80Tai, 99Kno].

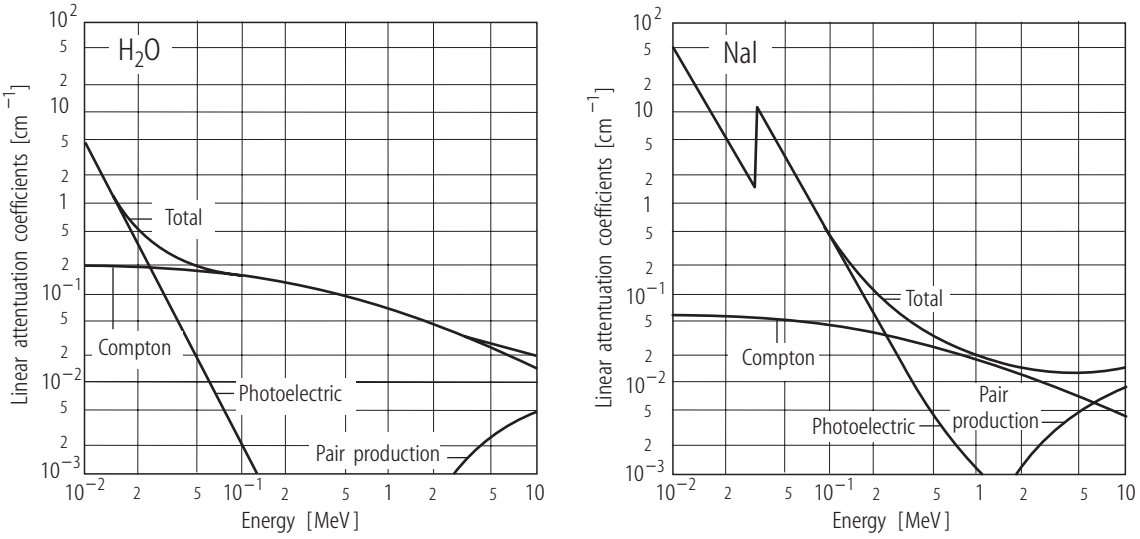

Fig. 10.33. Linear attenuation coefficient of H_2O and NaI.

The photoelectric capture predominates for low photon energies and the photons are absorbed much more strongly in high-Z materials than in low-Z materials. If the incident photon is absorbed by photoelectric effect in a detector, the resulting pulse contributes to the so-called full absorption peak or photo-peak, which provides the key information about the energy and the intensity of the incident photon radiation. If the photon undergoes Compton scattering, the resulting pulse contributes to the so-called Compton continuum of the detector spectrum which consists of two components: if the Compton scattering occurs inside the detector the resulting pulse contributes to the detector-specific Compton continuum which covers according to the energy of the scattered electron the energy range from zero for $\theta = 0°$ up to the so-called Compton edge for $\theta = 180°$. If on the other hand the Compton scattering occurs in the environment and the scattered photon is subsequently absorbed in the detector, then the resulting pulse contributes to the environment-specific Compton continuum which covers the energy range from the so-called backscatter-peak for $\theta = 180°$ up to the photo-peak for $\theta = 0°$. It is important to know that anticoincidence techniques can reduce only the detector-specific Compton continuum but not the environment-specific Compton continuum. More detailed information about photon interactions is given in Section 3.5.2.3.

Energy resolution

The energy resolution of a detector describes its ability to distinguish between photon energies. When exposed to a radioactive source, the detection system processes a number of monoenergetic photons, which results in a spectrum consisting of the photo peak and the Compton continua. For illustration Fig. 10.34 and Fig. 10.35 show the spectra of a NaI(Tl) scintillation detector (see Section 10.3.2.4.4.1) for low-energy photons (5.9 keV K_α X-rays from ^{55}Fe) and for high-energy photons (662 keV γ-rays from ^{137}Cs), respectively. The low-energy photons are fully absorbed in the detector because at 5.9 keV the probability for photoelectric absorption is more than two orders of magnitude higher than the probability for Compton scattering (Fig. 10.33). On the other hand, the high energy photons undergo mainly Compton scattering in the detector because at 662 keV the probability for photoelectric absorption is one order of magnitude less than that for Compton scattering. Thus, in the spectrum for low-energy photons there is only the photo peak whereas in the spectrum of high-energy photons there is in addition a broad Compton continuum including the backscatter peak and the Compton edge. Ideally, all fully absorbed monoenergetic photons would be assigned exactly the same pulse height (or channel) in the measured spectrum. However, the photo-peak in the measured spectrum is a distribution of pulse heights with a peak width that reflects the detector resolution. The full width at half maximum (FWHM) of the photo-peak is used to characterise the resolution of the detector. The FWHM is the energy width of the distribution at half the maximum of the photo-peak when the background has been subtracted. For low-resolution detectors, such as scintillation detectors, resolution is defined as the FWHM divided by the photo-peak energy, and is usually expressed as a percentage. The 662 keV gamma ray from ^{137}Cs is usually used as the reference for this purpose.

For high-resolution semiconductor detectors, the energy resolution is usually specified as the FWHM (keV or eV) for a specified energy. Manufacturers normally also provide the width of the photo-peak at one-tenth and one-fiftieth of the maximum, with reference values for the 1.332 MeV gamma ray from ^{60}Co or the 122 keV gamma ray from ^{57}Co, depending on the type of detector.

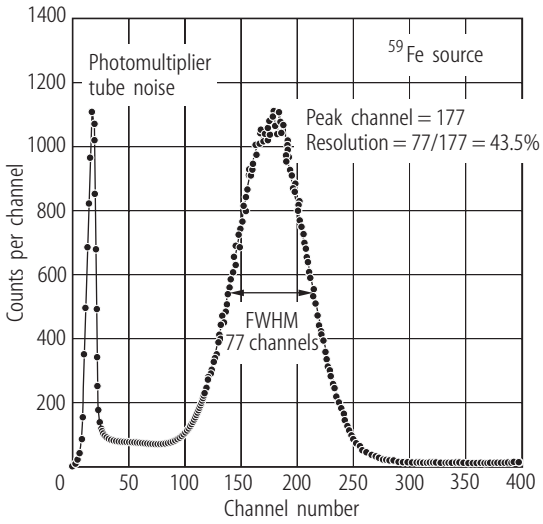

Fig. 10.34. Spectrum of a NaI(Tl) scintillation detector for low-energy photons (5.9 keV K_α X-rays from ^{55}Fe).

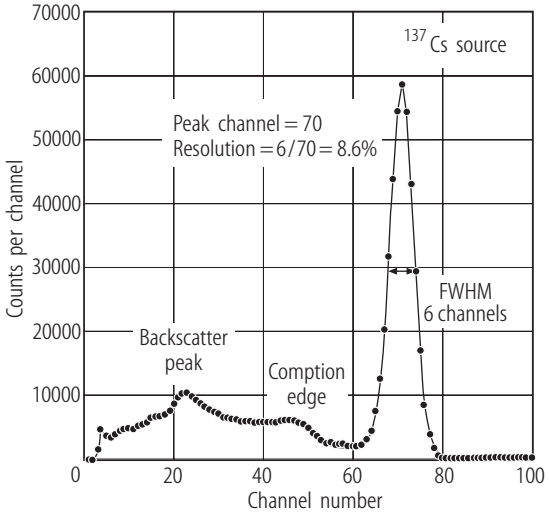

Fig. 10.35. Spectrum of a NaI(Tl) scintillation detector for high-energy photons (662 keV γ-rays from ^{137}Cs).

Detection efficiency

The detection efficiency is defined as the ratio of the number of photons detected to the number of photons emitted by a radiation source during a given time interval. The detection efficiency is made up by four factors:

1. *Geometrical attenuation factor*: the fraction of all emitted photons which are emitted in the direction of the sensitive volume of the detector, depending on the solid angle covered by the detector with respect to the source.
2. *Material attenuation factor*: the fraction of those photons emitted in the direction of the sensitive volume, which actually reach it, depending on the attenuation of the material in between the source and the detector.
3. *Interaction efficiency*: the fraction of photons reaching the sensitive volume that react with it, depending on the attenuation of the detector material.
4. *Data recording efficiency*: the fraction of photons interacting with the sensitive volume, which produce recorded events, depending on the type of recording (i.e. photo-peak counting or total counting) and the data acquisition system.

10.3.2.4 Equipment

10.3.2.4.1 Detectors

10.3.2.4.1.1 Scintillation detectors (see also Section 10.1.3)

There are three groups of scintillation detectors: crystals, glasses and gases. For *in vivo* measurements, however, only crystal type scintillation detectors are applied. Each photon, which interacts with the sensitive volume of the crystal, generates a single scintillation pulse. This is a very weak pulse, typically consisting of less than 1000 photons of few eV, so it has to be viewed by a highly sensitive photo-multiplier tube (PMT) and the whole assembly must be enclosed in a light-tight housing to isolate the scintillation from the ambient light. The characteristic properties of some selected scintillation materials are summarized in Table 10.14.

Table 10.14. Properties of NaI(Tl), CsI(Tl), $Bi_4Ge_3O_{12}$, and organic (Polystyrenetetraphenylbuta-diene) scintillators.

Property	NaI(Tl)	CsI(Tl)	$Bi_4Ge_3O_{12}$	Organic
Density [g/cm^3]	3.67	4.51	7.13	1.0
Light output relative to NaI(Tl)	1	0.45	0.12 - 0.20	0.14
Wavelength of maximum emission [nm]	415	550	480	450
Decay constant [μs]	0.23	1.0	0.3	0.005
Hygroscopic	Yes	No	No	No
Energy resolution at 662 keV [FWHM in %]	7 - 10	10 - 12	10 - 12	25 - 50

Sodium iodide activated with thallium (Nal(Tl)) provides the best properties with respect to light output, decay constant and energy resolution. However, NaI(Tl) is hygroscopic, and absorption of water results in a loss of energy resolution. So these crystals must be placed in gas-tight housings. A typical design of a NaI(Tl) scintillation detector is shown in Fig. 10.36. In between the crystal and the housing there is a MgO reflector and so the scintillation light can leave the crystal only via the optical window. Thus most of the scintillation light is collected on the photo cathode of the photomultiplier tube behind the optical window. A magnetic shield protects the photomultiplier tube in order to avoid deflection of the secondary electrons in the tube by external magnetic fields. Both the reflector and the magnetic shield make sure that the amplitude of the output signal is proportional to the energy absorbed in the NaI(Tl) crystal.

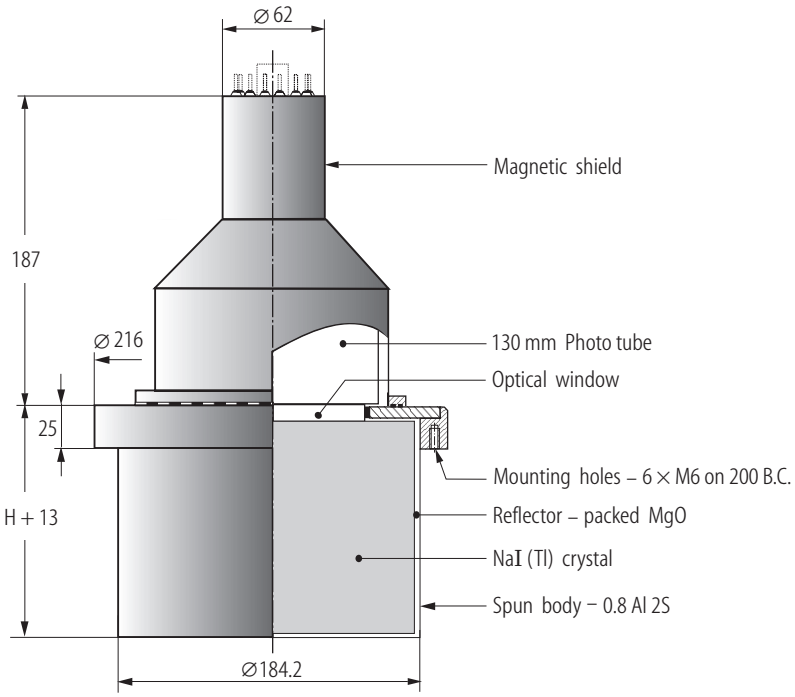

Fig. 10.36. Typical design of a NaI(Tl) scintillation detector (Harshaw matched window assembly with crystal dimensions: 178 mm ∅; 130 mm height).

Caesium iodide activated with thallium (CsI(Tl)) can also be used as scintillator material, but the light output is smaller and thus the energy resolution is not as good as that of NaI(Tl). So CsI(Tl) crystals are not commonly used for spectrometric measurements but they are frequently used as anticoincidence detectors in order to reduce the background of NaI(Tl) crystals, this requiring high efficiency but no high-energy resolution. The combination of NaI(Tl) and CsI(Tl) crystals as a dual phosphor sandwich (phoswich) allows for high sensitive detection of low-energy photons (see Section 10.3.2.4.3.2).

Because of the poor energy resolution of the scintillation detectors the photo peaks are relatively broad and thus the background prediction can be difficult, especially in the low-energy region. This is illustrated by Fig. 10.37 which shows the spectrum of a NaI(Tl)/CsI(Tl) phoswich detector for a subject with 0.25 kBq ^{241}Am in the liver, 1.5 kBq ^{241}Am in the skeleton and 12 kBq ^{137}Cs in the whole body. The photo peak due to the X-rays of ^{137m}Ba (daughter of ^{137}Cs) is overlapping to some extend the photo peak due to the γ-rays of ^{241}Am, and thus the separation of the photo peaks from each other and from the Compton continuum requires high sophisticated spectrum evaluation procedures (see Section 10.3.2.5).

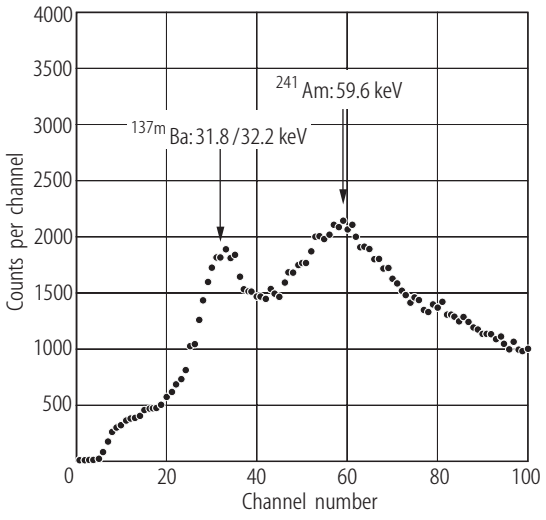

Fig. 10.37. Spectrum of a NaI(Tl)/CsI(Tl) phoswich detector (Harshaw 208 mm ∅ matched window assembly with 1 mm thick NaI(Tl) crystal and 51 mm thick CsI(Tl) crystal) for a subject with 0.25 kBq ^{241}Am in the liver, 1.5 kBq ^{241}Am in the skeleton and 12 kBq ^{137}Cs in the whole body (detector arranged over the liver, measuring time 2000 s).

Bismuth germanate ($Bi_4Ge_30_{12}$), often abbreviated to BGO, provides the highest efficiency of all available scintillation materials because of its high density and effective atomic number. The energy resolution, however, is relative poor and so BGO is applied only in those cases where small detectors with high photo peak efficiency are required, as for example wound measurements.

Organic scintillation detectors
Solutions of organic liquids [61Lan], and solid organic scintillators [62Bur], have also been used for *in vivo* measurement applications. Solid organic scintillators can be made by impregnating plastic materials with anthracene. They can be made in very large sizes (e.g. $60 \times 40 \times 10$ cm^3) but require several photomultiplier tubes to achieve even a modest energy resolution, and in consequence have not been widely adopted for radiological protection purposes. They could be considered only where the interest was in a single nuclide, or in a mixture whose composition was reliably known, and where interference from the body's natural ^{40}K could be either neglected or inferred from measurements prior to the subject's exposure. Organic scintillators can also be incorporated into liquid solvents; geometries approaching 4π can be produced with such solutions contained in annular tanks, but they suffer from the same restrictions as organic scintillators.

Organic scintillation detectors have almost the same photon absorption behaviour as soft tissue and thus they can be applied for direct assessment of the actual internal dose rate due to incorporated γ-emitting radionuclides [95Doe].

10.3.2.4.1.2 Semiconductor detectors

Semiconductor detectors are solid-state ionisation chambers, the principle of which being described in detail in Section 10.1.4 and elsewhere [92Del, 99Kno, 80Tai]. For *in vivo* measurements most commonly Germanium detectors are used, starting in former times with Li drifted Germanium detectors (Ge(Li)), which have been replaced since 1976 by high purity Germanium detectors (HPGe) [76Fal]. In the eighties mainly p-type HPGe crystals have been used. These crystals have a lithium diffusion zone to form the n-contact, which results in an insensitive layer of about 0.6 mm at the crystal surface. So only photons with energy higher than about 50 keV could be detected. Since the nineties also n-type detectors are been applied which have a boron ion implantation to form the p-contact. The implantation results in a very thin insensitive layer (0.3 μm) at the front of the crystal, thus allowing also for measurement of low-energy photons with energies of several keV.

Semiconductor detectors have major advantages in energy resolution, the FWHM being typically below 0.6 keV for low energy photons or 2 keV for high energy photons, respectively (Table 10.15). Thus, semiconductor detectors allow almost unambiguous identification of the radionuclides in a mixture, but most of them are inconvenient in that they need cooling to liquid nitrogen temperatures. High purity germanium (HPGe) detectors can tolerate cycles to room temperature but need cooling during operation. Furthermore, many semiconductor detectors are available only in fairly small sizes, so that their geometrical efficiency is small as compared to inorganic crystals and other scintillators. Compact arrays of three to six detectors are becoming standard for monitoring contamination in specific organs, such as the lungs.

Miniature semiconductor detectors, in particular those using cadmium telluride (CdTe) operating at room temperatures, are becoming increasingly available. CdTe detectors offer high sensitivity for detection of low energy photons. Their small size (approximately 10 mm in diameter and 2 mm thick) makes them ideal for localized wound monitoring.

Table 10.15. Properties of some selected semiconductor detector materials.

Property	Si	Ge	CdTe
Density [g/cm^3]	2.33	5.33	6.06
Band gap at 300 K [eV]	1.12	0.67	1.47
Energy per electron-hole pair at 77 K [eV]	3.61	2.98	4.43
Requires cooling	Yes[1)]	Yes	No
Energy resolution at 5.9 keV [FWHM in keV]		0.6	
Energy resolution at 1332 keV [FWHM in keV]		1.8	

1) If high resolution is required

The excellent energy resolution of HPGe detectors is illustrated by Fig. 10.38., which shows the spectrum for a subject with 0.25 kBq ^{241}Am in the liver, 1.5 kBq ^{241}Am in the skeleton and 12 kBq ^{137}Cs in the whole body. A comparison of this spectrum with the corresponding phoswich spectrum measured at the same subject in the same geometry at almost the same time (Fig. 10.37) reveals the major advantage of the HPGe detectors especially for the *in vivo* measurement of low-energy photon emitters.

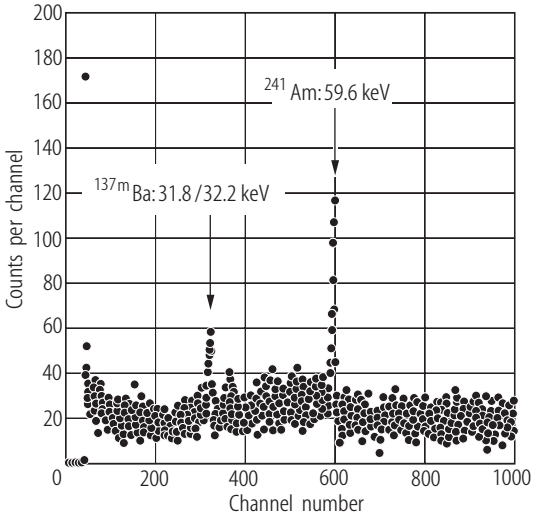

Fig. 10.38. Spectrum of a HPGe detector (Silena 50 % coaxial n-type HPGe crystal) for a subject with 0.25 kBq ^{241}Am in the liver, 1.5 kBq ^{241}Am in the skeleton and 12 kBq ^{137}Cs in the whole body (detector arranged over the liver, measuring time 2000 s).

10.3.2.4.1.3 Gas-filled detectors

There are three types of gas-filled detectors used for radiation protection measurements: Geiger-Müller tubes for counting of absorption events, ionisation chambers for dosimetry, and proportional counters for spectrometry. Large-area proportional counters with anticoincidence guard layers offer energy resolutions intermediate between those of scintillation counters and semiconductor detectors and, with acceptable detection efficiency at energies below 30 keV, they were in former times seen as the most profitable approach to the assessment of plutonium in lungs. Several designs were produced by individual laboratories using argon-methane or xenon-methane counting gas at normal or high pressure. The energy resolution was 13-15 % and the absorption probability was 30-85 % for the 13.6 and 17.2 keV uranium L X-rays from the decay of ^{239}Pu. High sophisticated designs were developed using full space anti-coincidence techniques for background suppression [76Sch]. However, the proportional counters fell into disuse with the development of the phoswich, which offered greater sensitivity and robustness.

10.3.2.4.2 Electronics (see also Section 10.1.3)

Electronic equipment is required to extract, amplify and sort electrical signals from the detector, converting them ultimately into a pulse-height distribution. It therefore includes a chain of preamplifier and main amplifier for pulse shaping and amplification followed by an analogue-to-digital converter and multi-channel analyzer for pulse height analysis; besides, units with specialized functions are required for phoswich detectors, or for controlling the movement of detectors scanning, high voltage power supplies, etc.

Preamplifier
The preamplifier being located close to the detector serves as a gain stabiliser and an impedance matcher. For scintillation detectors mainly voltage-sensitive preamplifier is used whereas for semiconductor detectors charge-sensitive preamplifiers are preferred. The preamplifier adds no or little amplification to the signal but it enables the signal to pass without loss of information through a coaxial cable to the main amplifier, which in general is located out of the shielding in several meters distance from the detector.

Main amplifier
The main amplifier serves for amplification and proper shaping of the pulses from the preamplifier. Modern amplifiers provide many functions for smoothing and shaping of the pulses by integration and differentiation, baseline restoration, pole-zero adjustment and linear amplification, the gain varying from a factor 10 to 5000. The output signal can be chosen to be unipolar (either positive or negative) or bipolar (first positive and then negative), the standard for spectroscopic applications being a positive unipolar pulse with amplitude up to 10 V. The length of the pulses is controlled by the shaping time constants and should not exceed 10 μs in order to avoid superposition of pulses at higher count rates which would result in broadening of the photo peaks and thus in a loss of energy resolution of the detector system.

Pulse-height analysis
For determination of the amplitude the pulses are first digitised by an analogue-to-digital converter (ADC) and then fed into a multichannel analyser (MCA). The MCA reads the pulses according to their height into a memory consisting of a certain number of channels, thus generating a spectrum i.e. a frequency distribution of the pulses as a function of their amplitude. The total number of channels per spectrum is defined by the width of the photo peaks. It should be large enough to provide full information about the peak shape in order to allow for proper separation of the photo peak from the background continuum or from overlapping photo peaks due to other radionuclides, respectively. On the other hand the number of channels should not be too large in order to have a sufficient number of pulses per channel or good counting statistics, respectively. For scintillation detectors 0.25k (256) channels are sufficient to cover the energy range from zero to 3000 keV, whereas for HPGE detectors up to 8k (8096) channels may be required to provide full information in this energy range.

At present time, both ADCs and MCAs are available as plug-in components of personal computers and customized computer codes for the qualitative and quantitative analysis of the measured spectra are available for all gamma spectrometry systems. The computer codes include basic functions such as background subtraction, and also more ambitious operations such as adjustment for instrumental drift, resolution of a spectrum into its several components by linear regression analysis and peak search, evaluation and identification procedures (see Section 10.3.2.5).

10.3.2.4.3 Shielding

The purpose of shielding is first of all to reduce the background radiation to the level necessary for the sensitivity required; but also to reduce perturbations in the counter background response, which occur because the subject's body distorts the ambient radiation field through absorption, scattering and other processes. The background is governed by cosmic radiation and the radiation of radioactive materials present in the local environment (see Chapter 11). The cosmic radiation consists primarily of charged particles of solar or galactic origin, which produce mesons, electrons, photons and activation products such as ^{7}Be or ^{14}N and

^{16}O due to interaction with the earth atmosphere. The radioactivity in the local environment is mainly due to natural uranium and ^{40}K, but also due to man-made ^{137}Cs from the nuclear weapons fallout and the Chernobyl accident, respectively. Also airborne activity such as ^{222}Rn and ^{220}Rn progeny may contribute significantly to the background radiation in the environment of the detector device. In addition, radionuclides in the detector device itself may give rise for some background components, i.e. ^{60}Co in steel components, uranium in aluminium and beryllium components, and ^{40}K in photomultiplier tubes.

The background may be characterized by the background index that gives the count rate per unit detector volume, typically in units of counts per minute per cm^3 over the energy range from 200 keV to 2 MeV. The reduction of the background is characterized by the background reduction factor indicating the ratio of count rates measured with a detector in a well defined energy range without and with applying a certain procedure for background reduction, as for example outside and inside a shielding room.

In principle, there are passive and active methods for background reduction: the passive methods are based on the absorption of environmental radiation with appropriate shielding materials and/or on the selection of construction materials with very low intrinsic radioactivity in the environment of the detector device whereas the active methods are making use of special anticoincidence techniques for reducing the detector specific background signal.

10.3.2.4.3.1 Passive shielding

The requirements for primary shielding materials are: high attenuation of gamma rays, requiring high atomic number and density; freedom from unacceptable concentrations of natural or artificial radionuclides; and suitable mechanical properties for fabrication and assembly. Steel or lead are most commonly used. If lead is chosen, there will be characteristic X-rays, induced by ambient radiation or by the subject's gamma-ray emissions; if these interfere in a critical energy region, they may be removed through an inner lining of a few mm of cadmium or tin, with the ensuing Cd or Sn X-rays eliminated if necessary by a further lining of steel or copper. For major installations typical thicknesses for the primary material are 5-10 cm lead or 10-20 cm steel. Those thicknesses seem to be optimum due to the fact that the background from the environment is about two orders of magnitude higher than the background from the subject due to the natural ^{40}K in the body. So it is making no sense to reduce the environmental background far below the background from the subject. Thus, a background reduction factor of 100 seems to be reasonable with respect to *in vivo* measurements in the energy range up to about 3000 keV. Such a background reduction factor is achieved for example by 14.6 cm steel (Table 10.16). Behind the shielding the environmental radiation is scattered down to a broad Compton continuum with a maximum around 200 keV. The Compton continuum may be attenuated by a factor of 100 with an inner lining of about 5 mm Pb. In the Pb lining, however, characteristic X-rays are produced with energy between 72 and 88 keV ($K_{\alpha 1}$ at about 75 keV). These X-rays then may be absorbed by an additional inner lining of about 2 mm Sn, and the X-rays from the Sn ($K_{\alpha 1}$ at about 25 keV) then may be absorbed by a third inner lining of about 0.25 mm Cu, this being the principle of the so-called "graded *Z* lining" which provide optimum shielding for *in vivo* measurements (Table 10.16).

Table 10.16. Design parameters for a "graded *Z* shielding".

Critical radiation	Reference energy [keV]	Absorption material	Linear absorption coefficient [cm^{-1}]	1 % thickness [cm]
Background photons	3000	Fe	0.315	14.6
Compton scattered photons from Fe	200	Pb	10.7	0.43
X-rays from Pb ($K_{\alpha 1}$)	75	Sn	25	0.18
X-rays from Sn ($K_{\alpha 1}$)	25	Cu	180	0.025

Shielded room

The most effective, convenient arrangement is a wholly shielded enclosure, to accommodate both the subject and the detector system. For a given thickness of the chosen shielding material, this design offers the greatest reduction in background and it offers also the smallest dependence of background response on body size.

Occasionally, subjects may react to isolation in a shielded room; such instances are much rarer where access to the counter is via an open shielded labyrinth rather than through massive hinged or sliding doors. In practice the background reduction factors are smaller than expected from the theoretical consideration above, mainly due to scattering of high energy photons (E_γ>3000 keV) down into the energy range of *in vivo* counting (Table 10.17).

Table 10.17. Shielding parameters for some selected shielded rooms for *in vivo* measurement devices

Shielding materials	Background reduction factor	Background index [cpm/cm^3]	Reference
70 cm silica sand, 0.3 cm Pb, 0.04 cm Cd, 0.1 cm Cu, 0.55 cm plastic	73	0.43	85Sch
15 cm Fe, 1 cm Pb, 0.2 cm Fe	100	0.36	85Sum
15 cm Fe, 0.9 cm Pb	40 - 57	0.34	61Kie

Partial shielding

Some installations comprise more open structures, which eliminate direct paths for radiation between the detector and the laboratory. Examples are the "shadow shield" design used for assessing whole-body radioactivity in which the subject lies on a bed moving under a fixed detector in a central turret. Other arrangements embodying the same principle can be devised to assess the radioactivity of individual organs or regions. In another simple arrangement the detector and the back of a chair or bed holding the subject are shielded for the investigation of radioactive deposits in larger regions. With all partially shielded counters the background response below 200 keV is likely to be much larger than in a shielded room, because they respond to photons scattered by the subject into the detector. For this reason a shielded room is essential for the sensitive assessment of low-energy photon emitters. More information about shielding is given for example in the IAEA "Directory of whole-body radioactive monitoring" [70IAE].

In addition to the shielding of the environmental radiation it is very important that all materials in the detector systems, the mounting facilities and the shielding are selected for low level of intrinsic radioactivity. Also the natural radioactivity in the construction materials of the surrounding building is important for the background. The natural activity concentration of ^{40}K can vary in between 200 Bq/kg and 800 Bq/kg in bricks and 320 Bq/kg and 800 Bq/kg in cement, respectively [92Zik]. Thus, there is a large potential for background reduction by proper selection of the construction materials. Moreover it is important to minimise the amount of material close to the detector system in order to minimise the background component due to Compton scattering in the direct vicinity of the detectors. Last but not least there is a need for air filtration in order to reduce the background component due to airborne radioactive materials.

10.3.2.4.3.2 Active methods

There is different kind of active methods for the reduction of the detector background signal, most of them being based on anticoincidence techniques. Firstly this technique was applied for proportional counters in order to reduce the background due to β particles or Compton electrons from the environment. For this purpose the counting volume of the proportional counter was surrounded by guard counters and all coincident absorption events in both the counting volume and one of the guard counters were discriminated. Thus only the events due to photoelectric absorption in the counting volume were processed, this resulting in very good detection features especially for low energy photons such as the plutonium L X-rays. On the other hand the sensitivity of these detectors for photons with higher energy as for example the 59.6 keV γ-rays of ^{241}Am is very low, even when the proportional counters were operated with heavy counting gases such as Xe under high pressure of 2 or 3 bar. However, for *in vivo* measurement of plutonium via the L X-rays it is essential to measure simultaneously the ^{241}Am activity present, because the L X-ray yield of ^{241}Am is one order of magnitude higher than that of plutonium. The energy resolution of the proportional counters does not allow for discrimination of the ^{241}Am L X-rays

from the plutonium L X-rays and so the contribution from ^{241}Am must be determined by measurement of ^{241}Am via the 59.6 keV γ-rays in the same measuring geometry. It was mainly due to this reason that the proportional counters were replaced in most laboratories by the phoswich detectors, which were commercially available since the late sixties.

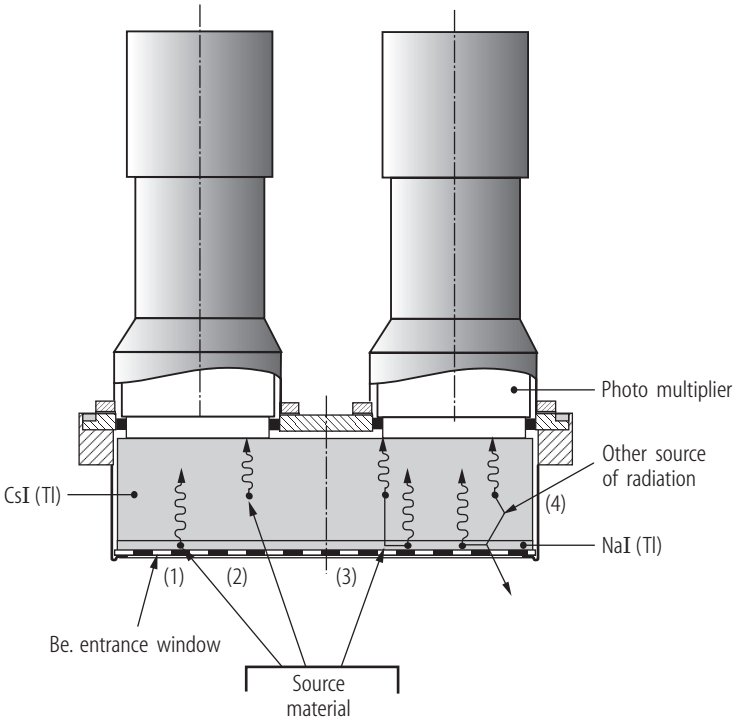

Fig. 10.39. Measuring principle of a phoswich detector.

The phoswich detector has been developed by Laurer for the *in vivo* measurement of low energy photon emitters such as ^{210}Pb, ^{239}Pu and ^{241}Am [68Lau]. The detector consists of a large area NaI(Tl) crystal the thickness of which being just enough to fully absorb the low energy photons (typically 1-3 mm). The NaI(Tl) crystal is backed by a CsI(Tl) crystal for the detection of scattered photons due to Compton effects in the NaI(Tl) crystal (Fig. 10.39). The photomultiplier tubes detect the scintillation light from both crystals. However, because of the different scintillation decay times of the materials, it is possible to assess by pulse shaping techniques whether the scintillation light is originating from the NaI(Tl) crystal, the CsI(Tl) crystal or from both crystals. Thus it is possible to discriminate the Compton scattering events (in both crystals) from the full absorption events, this resulting in a significant reduction of the detector specific Compton continuum of the NaI(Tl) crystal. When comparing the count rates of a phoswich detector in the low energy range (10 - 100 keV) with and without applying the pulse shape discrimination technique a reduction of about one order of magnitude is observed. This figure, however, does not correspond to the actual reduction of the Compton continuum from the NaI(Tl) crystal because most of the scintillations detected by the photomultipliers are due to absorption events in the CsI(Tl) crystal only. Actually the reduction of the NaI(Tl) Compton continuum is less than a factor 2 because the CsI(Tl) anti Compton shield covers less than a 2π space angle.

Phoswich detectors provide good detection features for low energy photon emitters if no high-energy photon emitters such as ^{137}Cs are present. Compton continuum, backscatter peaks and characteristic X-ray peaks due to those high-energetic emitters may influence the spectrum in the low energy region significantly, this giving rise for problems in background prediction.

10.3.2.5 Spectrum evaluation

The interpretation of a photon-energy spectrum of body radioactivity will involve initially the identification of radionuclides responsible for its individual features. The next stage, unless the spectrum is dominated by the contributions from a single radionuclide, will generally involve resolution into the constituent components. In a further process, the response attributable to a particular contributor will be translated into an estimate of body or organ radioactivity; this is accomplished by reference to a spectrum representing a known radioactivity of the nuclide measured in the same conditions.

Methods of deconvoluting photon-energy spectra of body radioactivity do not differ in principle from those applied in X- and gamma-ray spectrometry generally, except that account must often be taken of the effect on spectral shape of scatter in a large attenuating mass. The process is at its simplest in the estimation of peak areas from semiconductor detectors. The good energy resolution of such instruments allows the effective background response underlying a spectral peak to be reliably deduced from the adjacent continuum.

In the case of scintillation counters, the width of spectral peaks makes this approach often inapplicable especially in case of multiple peaks. It will generally be necessary to first subtract an appropriate spectrum of counter background and a more rigorous analytical procedure will generally be required.

The activity of the given radionuclide (q) can be expressed as follows

$$q = \frac{N}{t \cdot y \cdot \eta} \tag{10.3.2.3}$$

where N is the number of net counts in the full energy peak area,
t is the measuring time,
y is the yield of γ (or X)- ray,
η is the counting efficiency at the given energy for the respective measuring geometry

This is the most dominating evaluation method in gamma spectrometry.

Stripping method

When deconvolution of spectra from scintillation counters is required, a "stripping" process is sometimes followed. Reference spectra are derived for each nuclide present, each representing the response from known amounts of the nuclide in appropriate measuring geometry and in relevant absorbing media. The reference spectrum containing the peak with the highest energy is selected, and it is normalised to the subject's spectrum on the basis of count rate in an energy region where only that nuclide contributes. Subtraction of the normalised spectrum gives a residue representing the remaining components, which is treated in the same way. The activity of each radionuclide is calculated directly from the fraction of its reference spectrum, which must be subtracted. In principle, the process can be repeated until the residue consists of the response from a single nuclide only. In practice, unacceptable errors are likely to accumulate if the number of stages exceeds two or three, particularly in relation to minor components in a spectrum; moreover, the method will generally be inapplicable when the dominant peaks of different components overlap.

Linear regression analysis

A more satisfactory procedure in many situations is to adopt a method of linear regression analysis, to derive the proportions of each reference spectrum which, when combined, gives rise to the best fit to the subject's spectrum. Facilities for such analyses are embodied in several commercially available computer programmes for processing γ ray spectra; alternatively, they can be developed locally. Utilizing a much larger portion of the spectrum, instead of the restricted regions successively considered in the stripping process, this method gives improved statistical accuracy in the estimates of the various components; moreover, realistic estimates of this accuracy may be derived in the matrix-inversion procedures.

As with other methods of deconvolution, this approach has its limitations. In particular, it demands stability of the spectrometer during the measurement, especially if the nuclides present possess overlapping spectral features. It is also important that the locations of peaks in the subject's spectrum should coincide with those in the relevant reference spectra; where minor drifts occur between the measurements, adjustments can

often be made prior to the analysis if appropriate routines are available. However, the validity of the analysis depends also on the spectral shapes of the reference standards according with those of the corresponding components in the subject's spectrum.

This method is used practically exclusively in scintillation gamma spectrometry, however the procedure can be extended to the deconvolution of any kind of complex distribution of measured data. Such application is unfolding profile scanning data to quantify the measured distribution pattern in terms of activity deposited in different body regions or organs.

10.3.2.6 Measuring geometries

In principle, the *in vivo* measuring systems can be allocated to two different types of systems, namely geometry dependent and geometry independent systems. Here the geometry is defined as the detector configuration in relation to the photon-emitting source in the body.

10.3.2.6.1 Geometry depending systems

Static geometry

The most common kind of geometry dependent systems are those having detectors that are positioned close to the subject looking to specific organs or tissues. The advantages include high efficiency, better subject positioning and less space requirement for the system. The use of such a static geometry dependent system is extremely important in measuring low energy photons where the efficiency of the detection system needs to be maximized.

Isotopes of iodine, and also ^{99m}Tc may concentrate in the thyroid gland. The range of photon energies encountered is 27 keV (^{125}I) to several hundred keV. Some HPGe detectors used for assessment of actinides in lungs are of suitable diameter (ca. 50 mm) in relation to the size of the thyroid, and are large enough to provide adequate detection efficiency over most or all of this energy range. Alternatively, a planar germanium detector or thin NaI(Tl) crystal may be adopted for photon energies <100 keV, with thicker crystals, either NaI(Tl) or co-axial germanium detectors, used if necessary to secure efficient photon detection at high energies. More accurate assessment of an easily-detectable deposit would require better shielding, with the detector recessed in a suitable collimator.

Inhalation is the most common route for intake in occupationally exposed personnel, with the respiratory tract being the site of initial deposition. If the deposit persists for a sufficient time, monitoring of pulmonary activity may offer the most sensitive and reliable means of assessing the intake. Indeed, in the case of certain actinides which subsequently re-locate to organs absorbing virtually all low-energy photon emissions, it offers the only remotely practicable means of assessing an intake by external counting. A large-diameter (150-300 mm) stationary NaI(Tl) detector recessed in a cylindrical collimator may be used. The response would preferably be recorded in two locations, the detector viewing in turn the anterior and posterior surfaces of the thorax; ideally, if two such detectors were available, the measurements could proceed simultaneously. The sensitive measurement of pulmonary deposits of low-energy photon emitters (<100 keV) is most commonly required for ^{241}Am and for isotopes of uranium and plutonium. It requires equipment giving a better signal-to-background ratio than is provided by NaI(Tl) detectors. This is achieved either through partial suppression of background response as in the phoswich detector, or through the improved energy resolution offered by semiconductor detectors [00Lop]. Fig. 10.40 - Fig. 10.42 show as typical examples the arrangements of 2 phoswich detectors and 4 HPGe detectors as used in the Research Centre Karlsruhe for the *in vivo* measurement of low energy photon emitters in the lungs.

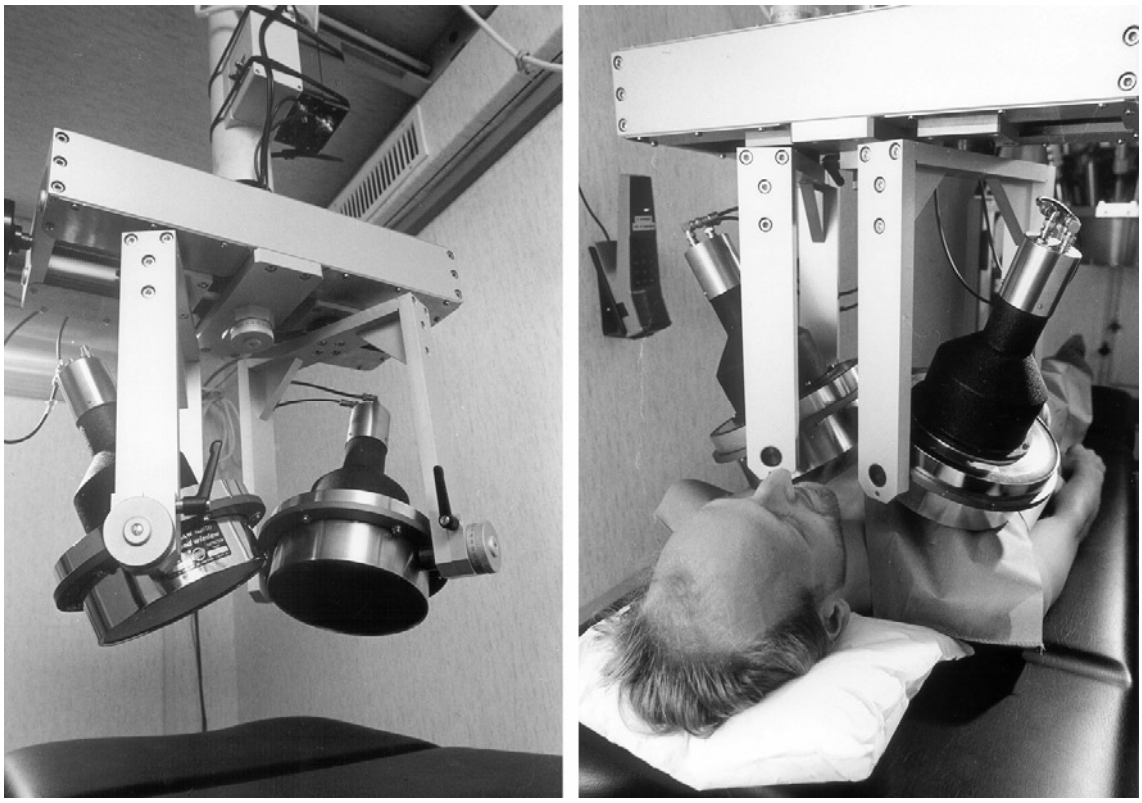

Fig. 10.40. Typical arrangement of 2 phoswich detectors (Harshaw 20 cm diam. 1 mm NaI(Tl) / 50 mm CsI(Tl) crystals) for in vivo measurement of low energy photon emitters in the lungs

Two other sites of deposition, which frequently attract specific interest, are bone and liver. Arrays of detectors viewing the skull have been employed to assess skeletal deposits of ^{210}Pb (47 keV photons) and ^{241}Am (59.6 keV). The levels of contamination in liver and skeleton may also be of interest in regard to their interfering contributions when lung deposits are assessed.

An extreme, but fairly common example of a localized deposit is the presence of poorly soluble radioactive material at the site of a puncture wound, investigated shortly after an accident, before important quantities have become systemic. With fission or activation products giving abundant and energetic photon emissions and with high limits of intake, improvised arrangements employing any spectrometrically suitable scintillation or semiconductor detector are likely to be satisfactory.

Profile scanning geometry

Another kind of geometry dependent systems is using moving detectors or subjects. The so-called scanning systems can be used for identifying the organ or tissue where the radionuclide in question is deposited. The so-called profile scanning systems are providing information on the activity distribution pattern in the body. Better spatial resolution can be obtained by using collimators in the front of the detectors however it can only be done at the expense of the counting efficiency. Profile scanning measurement may also point to the presence of surface contamination, which has to be removed.

It should be noted that profile scanning with simple slit-collimated detectors would often give reliable indications of the relevant sites of deposition, but that only a rough evaluation of that deposition can be obtained if a single detector viewing only one aspect of the body is employed. Quantitative assessment of radionuclide distribution by profile scanning requires either paired detectors or, if only one is available, separate traverses of the anterior and posterior surfaces, and further improvements may result if focused collimators are used and computer-aided evaluation techniques are applied.

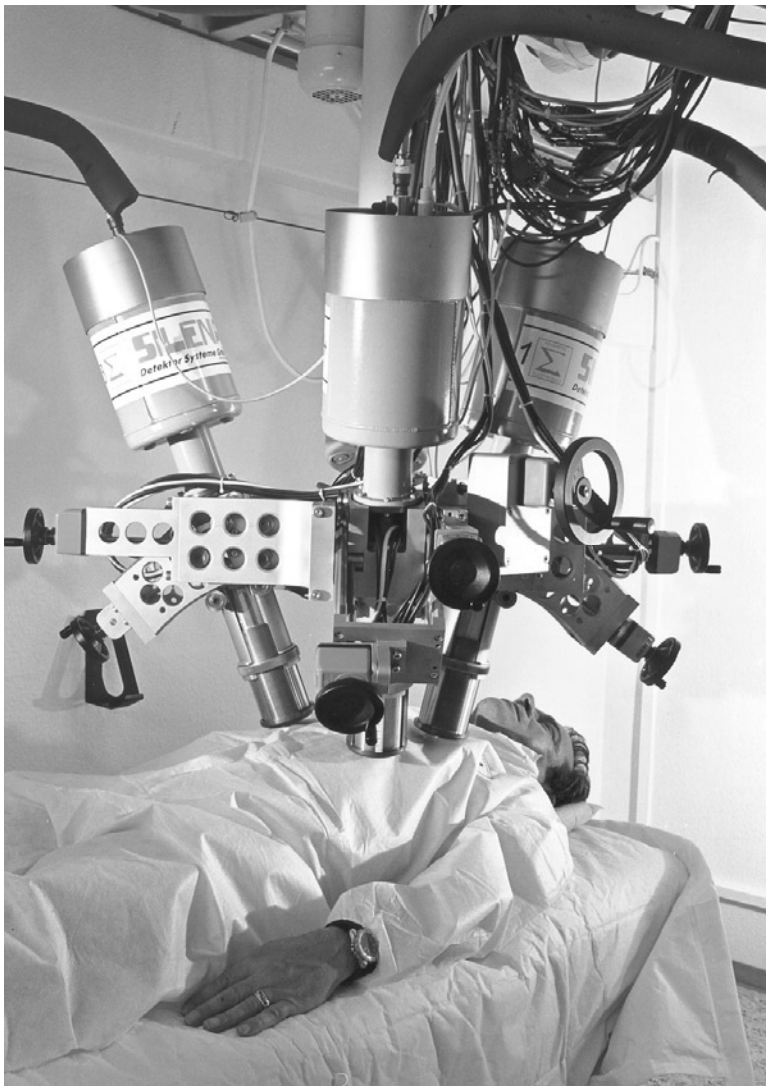

Fig. 10.41. Typical arrangement of 4 HPGe semiconductor detectors (Silena HPGe sandwich with 20 cm diam. planar p-type HPGe crystal backed by 50 % coaxial n-type HPGe crystal) for *in vivo* measurement of low energy photon emitters in the lungs.

10.3.2.6.2 Geometry independent systems

Geometry independent systems are characterized by the detectors being located in a certain distance from the subject to be measured, either above or below or both. In those arrangements the detectors have an almost uniform response for any distribution of gamma emitters in the body. Thus, arrangements characterized by this geometry independent feature were originally called as whole-body counter.

Arc geometry
This arrangement is capable of high accuracy if the levels of internal radioactivity and the space available inside a shielded room are sufficient. The subject lies on a curved frame forming the arc of a circle centered at the detector, so that all parts of the body are roughly equidistant from it. The detection efficiency is of course poor and, even with a large detector in a heavily shielded room, the technique will not generally be applicable to the determination of body burdens below several kBq; it would seldom be feasible with semiconductor detectors. In the context of radiological protection, therefore, the arc method will be used primarily in the investigation of established cases of internal contamination rather than as a regular means of control.

Chair geometry
In this arrangement the subject reclines in a tilted chair with the detector supported typically 0.4 m above the abdomen. The detector will commonly be a NaI(Tl) scintillator, e.g. 200 mm diameter × 100 mm, and in a heavily shielded room would be capable of detecting as little as 50 Bq of most common fission and activation products in a counting time of 15 min. Similar arrangements have been employed with semiconductor detectors. The response will however depend markedly on the location of the radioactive deposit, e.g. in the lungs or liver, may differ by a factor of two or more from that applying to material widely dispersed in the body. The potential for systematic error is accordingly much greater than with the arc technique, but this will be unimportant in many routine applications. Recently, fully automated chair type whole body counters have been developed providing very good detection features [02Sin]. The chair geometry is also applied in most of the mobile whole body counters used for monitoring of staff of nuclear power plants.

Scanning geometry
With this design of counter, the response is accumulated from a single detector while traversing the subject's length at a fixed distance above or below the supine body, or in some versions, in a corresponding disposition relative to the erect body. Alternatively, the supine subject may be moved in relation to a fixed detector. Accuracy will be improved if a second traverse is performed with the subject's posture reversed and the evaluation is based on the combined response in the two positions. When employing two detectors (one above and one below the supine subject), a more representative sample of the photon flux is obtained by moving the supine subject relative to the counters during accumulation of the spectrum.

However, while scanning arrangements can provide more uniform detection geometry compared with that given by most other configurations, they might not yield significantly greater accuracy than a well-designed multi detector array of stationary detectors. Useful indications of the distribution of a radionuclide within the body may be secured if the system can display a profile of the response according to position.

Stretcher geometry
An alternative approach, preserving the good detection efficiency given by the chair technique but offering improved uniformity of response, is to adopt a "stretcher" geometry, with the subject in a supine posture and several detectors distributed about the body. Commonly 4-8 detectors are employed, disposed above and below the stretcher so that their combined response is acceptably independent of the source distribution. Complete uniformity of efficiency is of course unattainable, however, for activity, which is not concentrated in small organs or regions, such an array can yield results for energetic (>100 keV) photon emitters accurate to within 20 % or better. Fig. 10.42 shows as an example a stretcher type whole body counter with 4 NaI(Tl) scintillation detectors as used in the Research Centre Karlsruhe for *in vivo* measurement of photon emitters with energy between 100 and 3000 keV.

Disadvantages are the need to provide several independently adjustable supporting mechanisms for the various detectors, and the requirement of a larger shielded room than would generally be necessary to accommodate only a chair.

Table 10.18. Comparison of various whole-body counter geometries

Geometry	Mechanical arrangement	Uniformity of response	Information on distribution	Sensitivity	MDA of ^{137}Cs. [Bq]
Arc	fixed	very good	no	low	300
Chair	fixed	poor	no	high	100
Static array	fixed	good	possible	high	70
Scanning (collimated detectors)	moving detector or moving bed	good	yes	high	100
Shadow shield	moving bed	good	yes	medium	130

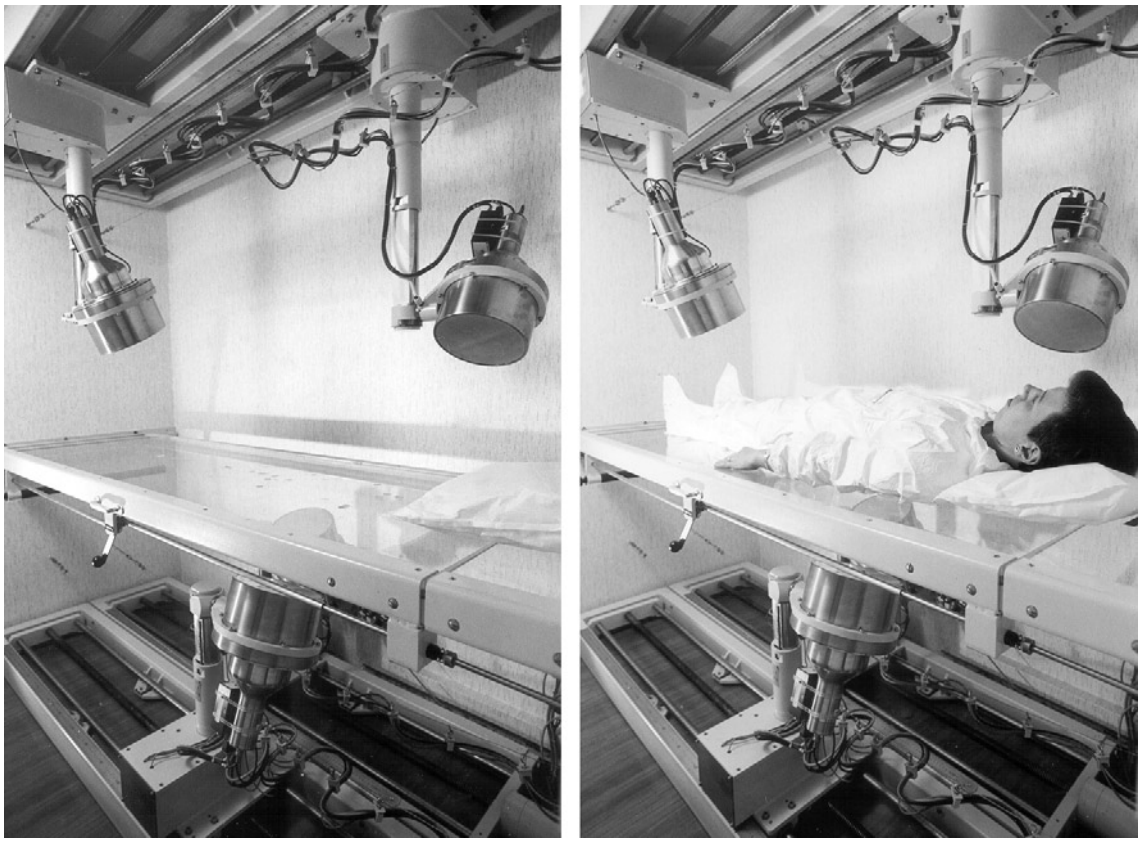

Fig. 10.42. Stretcher type whole body counter with 4 NaI(Tl) scintillation detectors (Bicron 20 cm diam. × 10 mm crystals) for *in vivo* measurement of medium energy photon emitters (100 - 3000 keV)

10.3.2.7 Calibration

The purpose of whole-body counter calibration is to determine the relationship between the detector response and the radioactivity in the body. Gamma emitting radionuclides can be characterised by the shape of their spectra or by the location of spectral peaks, which correspond to emitted photon energies. In certain circumstances, for example when spectra from scintillation counters are analyzed by least-squares fitting, it is essential to use the same nuclides for calibration as those to be measured. In the situations it may suffice to derive a calibration factor by interpolation of data measured individually for a series of monoenergetic photon emitters covering the energy regions of interest. With high-resolution semiconductor detectors, a single nuclide emitting photons at several energies, or a suitable mixture of nuclides, may be more convenient.

10.3.2.7.1 Energy calibration

As has already been mentioned energy calibration establishes the relationship between spectral peak location (channel number) and emitted gamma ray energy. This relationship may then be used to identify radionuclides from the location of their spectral peaks. Energy calibration is performed using radioactive sources emitting gamma rays with known energies. The gamma energies emitted by the calibration source(s) should cover the range of energies likely to be encountered during whole-body measurements.

Table 10.19 lists a selection of radionuclides suitable for calibration purposes. The analysis systems in modern whole-body counters automatically derive the energy calibration relationship using fitting routines and also plot the function for inspection.

Many software techniques require that the peak shape has to be characterised as a function of energy. Even if the software does not require it, peak shape is a useful tool both to confirm proper operation of the detector and to identify the presence of multiple nuclides with similar gamma energies. Peak shape calibration, characterised by FWHM (Full width at half maximum height), is usually performed at the same time and with the same spectrum as energy calibration.

Table 10.19. Characteristic parameters of radionuclides suitable for photon energy and efficiency calibration

Nuclide	Half-life	Photon emission		Nuclide	Half-life	Photon emission	
		Energy [keV]	Emission probability [%]			Energy [keV]	Emission probability [%]
^{55}Fe	2.73 y	5.89 (Mn Kα_2)	8.4			1274.54	99.94
		5.90 (Mn Kα_1)	16.6				
		6.49 (Mn Kβ_1)	3.4	^{137}Cs	30.0 y	661.66	85.0
^{241}Am	432.0 y	13.93 (Np Lα)	13.2	^{54}Mn	312.5 d	834.84	99.98
		17.61 (Np Lβ)	19.4				
		21.00 (Np Lγ)	4.9				
		26.35	2.4	^{46}Sc	83.80 d	889.28	99.98
		59.54	36.0			1120.55	99.99
^{109}Cd	463 d	88.03	3.65	^{60}Co	1925.5 d	1173.24	99.90
						1332.50	99.98
^{57}Co	271.84 d	122.06	85.59				
		136.47	10.58	^{88}Y	106.66 d	898.04	94.6
						1836.06	99.24
^{141}Ce	32.50 d	145.44	48.9				
				^{152}E	4939 d	121.78	28.37
^{139}Ce	137.65 d	165.85	80.0			244.69	7.51
						344.37	26.58
^{203}Hg	46.61 d	279.20	81.3			778.89	12.96
						963.38	14.62
^{51}Cr	27.71 d	320.08	9.58			1085.78	10.16
						1112.02	13.56
^{22}Na	950.4 d	511.00	180.7			1407.95	20.58

10.3.2.7.2 Efficiency calibration

Efficiency calibration allows one to convert the measured count rate in a region of the spectrum to the emission rate of the corresponding gamma photon of the radionuclide. Emission rate can then be converted to disintegration rate or activity using the probability of photon emission per decay. The conversion factor between count rate and activity is energy dependent and must be measured for the range of photon energies, which are expected to be present in the whole-body measurements. The variation in the efficiency factor as a function of photon energy may be obtained by simple interpolation between the measured points on the spectrum or by fitting an empirical function to the points. If one knows in advance the radionuclide to be measured, a situation frequently encountered in medical applications, then the efficiency factor is simply determined by using the same nuclide for calibration. In general, however, more complex spectral techniques are needed to derive efficiency factors for the spectra encountered in radiation protection applications. Different spectral analysis techniques should be applied to high or low-resolution detector systems.

To achieve accuracy in calibration the following factors must be observed:

- The same detector and hardware configuration should be used both for calibration and whole-body counting; the possible influence of necessary changes on the detection efficiency must be checked.
- Identical spectral analysis methods must be used.
- The source - detector geometry must be adequately simulated.
- The photon attenuation conditions applying in the body should be adequately reproduced

As a general rule the lower the energy of the photons to be detected the greater the care required to achieve a specified accuracy.

10.3.2.7.2.1 Point source calibration

This procedure may be adopted for whole-body counters whose “geometrical” counting efficiency shows little dependence on the location of the source, for example those disposed in distant arc geometry and in certain scanning arrangements. With the arc geometry, calibration accurate to within a few percent can be achieved with a standardised point source suspended in a tank of water or located between stacked plates of a solid absorber with comparable attenuation properties, the appropriate location of the source in the tank or stack is deduced from examination of the spectral shape and evaluation of the relative photon fluxes emerging from the subject's surfaces.

10.3.2.7.2.2 Phantom calibration

In practice systemic radionuclides tend not to be concentrated in a single anatomical region and such counters are generally calibrated, at least in the first instance, with the aid of whole-body phantoms simulating the human form and containing a standardised aqueous solution of the relevant nuclide. The most convenient general-purpose phantom is the so-called BOMAB (BOdy Manikin ABsorption) phantom, which consists of a collection of polyethylene vessels of circular or elliptical cross-section (Fig. 10.43). These are available commercially, or can be made by a workshop with experience of plastics. It is useful to have available two or three such phantoms with dimensions suitably scaled to represent individuals of different sizes; for intermediate physiques calibration factors may be derived by interpolation according to functions of anatomical parameters e.g. weight/height.

Fig. 10.43. The BOMAB phantom for simulation of homogeneous activity depositions in the whole body

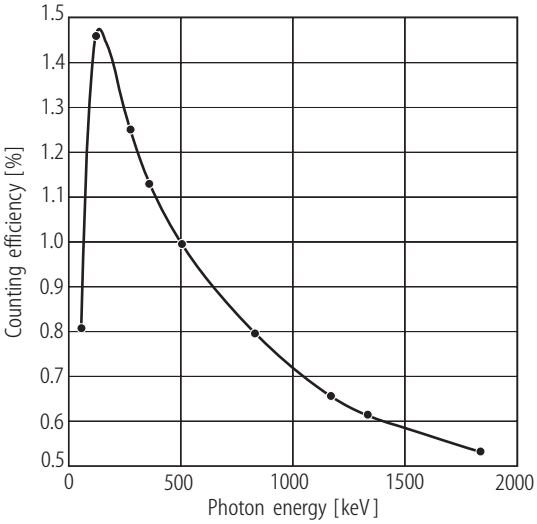

Fig. 10.44. Counting efficiency of a standard whole body counter (stretcher type with 4 NaI(Tl) scintillation detectors as shown in Fig. 10.43) for homogeneous activity depositions in the whole body according to calibration with the BOMAB phantom.

Alternatively makeshift arrangements, e.g. using plastic reagent bottles, may suffice; and in some situations more versatile in simulating specific physiques and postures (Bottle phantom). Conversely, much more elaborate whole-body phantoms (REMCAL, REMAB) can be purchased, some of them provided with discrete organs, which can be labelled independently of a dispersed deposit. Such complicated devices would ordinarily be required only in the calibration of equipment for assessment of deposits in specific organs. Recently, phantoms were developed which do need to be filled by water solution of radionuclides. Organic gels with dissolved radionuclides are used for the filling of BOMAB phantoms or large number of point sources is inserted into polyethylene bricks from which phantoms of different body height and weight could be easily built (IGOR). Comparison of various phantom characteristics is shown in Table 10.20

Table 10.20. Comparison of the characteristics of different phantoms used in whole-body counting.

Type of Phantom	Availability	Price	Versatility	Antropo-morphity	Handling	Decontamination
Bottles	very good	cheap	good	satisfactory	easy	not necessary
BOMAB	good	medium	bad	satisfactory	easy	difficult
REMCAL	good	very expensive	good	good	complicated	very difficult
REMAB	good	very expensive	good	good	complicated	very difficult
Presswood	very good	cheap	bad	bad	easy	not necessary

Besides phantoms for whole-body counting there are several phantom constructions simulating certain body regions such as thyroid in neck phantom (IAEA/ANSI neck phantom) or chest phantom containing organs like lungs, pulmonary lymph nodes, liver etc. (LLNL realistic chest phantom, JAERI phantom for Asian men). These latter phantoms were very sophisticatedly constructed which are especially suitable for calibration of low energy photon emitting radionuclides like transuranium elements deposited in the human respiratory tract. The LLNL chest phantom has been developed at the Lawrence Livermore National Laboratory and then manufactured by Humanoid Systems Inc. (Fig. 10.45). The phantom made from tissue equivalent materials represents the thorax of a male adult with 177 cm height and 76 kg weight. Lungs, tracheo-bronchial lymph nodes and the liver can be exchanged by active components with homogeneous deposition of plutonium and other low energy photon emitters. Overlay structures are also provided for the simulation of chest walls with different thickness (1.6 - 4.1 cm) and different muscle/adipose composition. At present there are 3 generations of the LLNL phantom, which are used as international standard for lung counter calibration [02Kra]. However, the LLNL phantom cannot be used for calibration for inhomogeneous deposition in the lungs or other organs. For this reason a second anthropomorpheous phantom has been provided by Humanoid Systems with the organs having a hole matrix for inserting small cylindrical sources in order to simulate any kind of inhomogeneous organ deposition (Fig. 10.46).

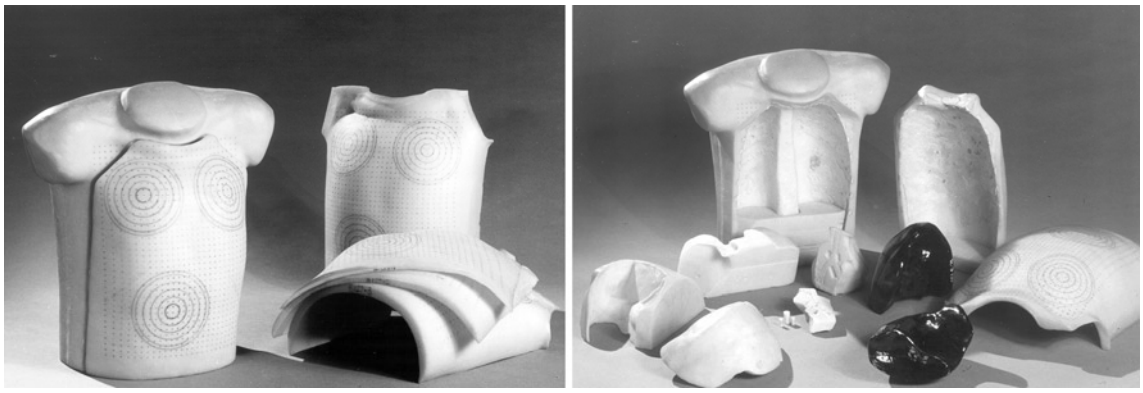

Fig. 10.45. The LLNL chest phantom for simulation of homogeneous activity depositions in the lungs, tracheo-bronchial lymph nodes and in the liver (Humanoid Systems Inc.)

Fig. 10.46. The "Fission product phantom" for simulation of activity depositions in all relevant organs of the trunk (Humanoid Systems Inc.)

10.3.2.7.2.3 *In vivo* calibration

On occasion, known activities of short-lived tracers have been administered to volunteers expressly in order to calibrate whole-body counters, e.g. ^{132}Cs and ^{42}K. It may sometimes be possible to make use of subjects who have received intakes in medical diagnosis or other metabolic studies. This would only be possible under supervision of ethics committee. If the measurement is delayed after intake of the tracer, e.g. to allow its distribution to stabilise, excreta voided in the interim may need to be collected and assessed for their content of radioactivity. When taking into account the loss of activity, the results of *in vivo* calibration are in very good agreement with the results of phantom calibration, as demonstrated by Kaul for ^{42}K [64 Kau].

10.3.2.7.2.4 Mathematical calibration

Methods of calibration using phantoms are relative methods; absolute methods do not require a radioactive standard for calibration, however standards must be used to confirm a calibration. Mathematical phantoms, using Monte Carlo method may be used for such calibration, as demonstrated by Mallet [95Mal]. The advantage of such phantoms is that any distribution of the radionuclide in the phantom could be used. However, thorough comparison of calculated examples with the measured values has to be performed as to ensure good quality of the mathematical phantom. It is especially important when low energy gamma emitters are subject of interest and the radionuclide in the body is non-homogeneously distributed, as shown by Hunt for some cases with ^{241}Am in the lungs and at the bone surface or with natural uranium in the lungs, respectively [03Hun].

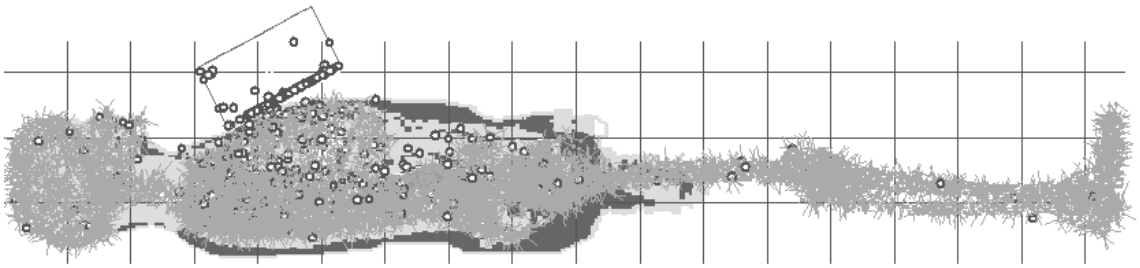

Fig. 10.47. The "Yale phantom" as used by Hunt for the Monte Carlo simulation of the radiation transport from the activity deposition in the body (i.e. ^{241}Am at the bone surface) to the detector outside the body (i.e. 8" × 4" NaI(Tl) scintillation detector over the lungs) [03Hun].

10.3.2.8 Uncertainties and detection limits

Generally, the uncertainties in the measurement are difficult to estimate. When activity levels are low and close to the limit of detection, uncertainties due to counting statistics may dominate the overall uncertainty. For radionuclides that are easily detected and present in sufficient quantity, uncertainties due to counting statistics will be small compared to other sources of uncertainty. Consideration must also be given to systematic uncertainties in other parts of the measurement procedure, e.g. calibration, or correction for body size of *in vivo* measurements, etc. Typically, the components of uncertainty are grouped in two categories: Type A comprises those components, which can be described by the Poisson distribution (i.e. counting error, to some extend also the variation of background signal and the variation of the subject positioning) whereas Type B comprises all other components (i.e. variation of body dimensions, overlaying structures, distribution of activity within the body, and the uncertainty of the calibration standard). The Type B components cannot be expressed in terms of Poisson statistics, and thus they cannot be associated with the Type A components in order to derive the total uncertainty of the measurement. Table 10.21 lists some typical values for the various components of uncertainty.

Table 10.21. Typical values for the components of uncertainty for the *in vivo* measurements of radionuclides emitting low, intermediate and high photon energy radiation

Source of uncertainty (Type)	Uncertainty (%)		
	Low photon energy E <20 keV	Intermediate photon energy 20 keV < E <100 keV	High photon energy E >100 keV
Counting statistics (A)	50 %	30 %	7 %
Variation of detector positioning (A)	20 %	5 %	<5 %
Variation of subject background (A)	50 %	10 %	<5 %
Variation in body dimensions (B)	50 %	12 %	7 %
Variation of overlaying structures (B)	30 %	15 %	12 %
Variation of activity distribution (B)	30 %	5 %	<5 %
Calibration (B)	5 %	5 %	5 %
Spectrum evaluation[1)] (B)	15 %	5 %	3 %

1) HPGe detector spectra

The statistical quantities for describing the Type A uncertainty and the corresponding detection limits are analogous to those used in all other kind of radioactivity measurement. Therefore, in recent years mainly the ISO definitions [98ISO] are applied for the calculation of uncertainties and detection limits of *in vivo* measurements. There are two basic terms being complementary to each other, i.e. *decision threshold* and *detection limit*.

Decision threshold
The decision threshold (frequently also referred to as *decision level* or *critical level*) is an a posteriori calculated value at which the decision can be made, whether the registered pulses include contributions from the body or are solely due to background. If this decision rule is observed, a wrong decision that there is a contribution from the body when actually only a background effect exists (Type I error), occurs with a well-defined probability α. By definition the decision threshold is given in terms of pulses but for practical application it is frequently transferred to the corresponding activity value.

Detection limit
The detection limit (frequently also referred to as *minimum detectable activity* or *lower limit of detection*) is an a priori calculated value, which specifies the minimum body contribution that can be detected by a defined measurement procedure. The detection limit is complementary to the decision threshold, i.e. when considering the detection limit the wrong decision that there exists only a background effect when there is in fact a contribution from the body (Type II error), occurs with a well-defined probability β. Thus, the detection limit is closely related to the decision threshold defined by the Type I error probability α. By definition the detection limit is given in terms of body or organ activity and it can be compared directly with guideline values.

The choice of the values of α and β depends on the aim of the measurement. For the purpose of radiation protection typically the values $\alpha = \beta = 0.05$ are used (i.e. 5% probability for both Type I and Type II errors). With these values the following formula for the decision threshold may be derived from the general concept given by Altshuler and Pasternack [63Alt]:

$$N_{DT} = 1.645 \cdot \sqrt{N_B \cdot \frac{t_S}{t_B}\left(1 + \frac{t_S}{t_B}\right)} \tag{10.3.2.4}$$

where
N_{DT} is the decision threshold in terms of net counts in the full energy peak region for $\alpha = \beta = 0.05$,
N_B is the total number of background counts in the full energy peak region,
t_B is the background measuring time,
t_S is the subject measuring time,

For the detection limit the generic formula derived by Currie [68Cur] may be used:

$$N_{DL} = 2.71 + 2 \cdot N_{DT} \tag{10.3.2.5}$$

where
N_{DL} is the detection limit in terms of net counts in the full energy peak region for $\alpha = \beta = 0.05$.

When the background count rate is high enough, Eq. (10.3.2.5) can be simplified and the following expression is derived for the detection limit:

$$q_{DL} = \frac{3.3}{t_S \cdot y \cdot \eta} \cdot \sqrt{N_B \cdot \frac{t_S}{t_B}\left(1 + \frac{t_S}{t_B}\right)} \tag{10.3.2.6}$$

where
q_{DL} is the detection limit in terms of body or organ activity for $\alpha = \beta = 0.05$
y is the yield of γ (or X)- ray,
η is the counting efficiency at the given energy for the respective measuring geometry

Table 10.22. Typical detection characteristics of a standard whole body counter (stretcher type with 4 NaI(Tl) scintillation detectors as shown in Fig. 10.40) for homogeneous depositions of some selected fission and activation products in the whole body (subject counting time t_S = 300 s; background counting time t_B = 1800 s)

Nuclide	Detected photon radiation		Counting efficiency η [%]	Background count rate N_B/t_B [cps]	Lower limit of detection [Bq]	
	Energy [keV]	Yield y [%]			Required (Table 10.12)	Achieved
^{57}Co	123	86	1.5	14.0	20000	60
^{137}Cs	662	85	0.9	7.4	10000	73
^{134}Cs	796	85	0.81	4.9	6000	66
^{60}Co	1173	100	0.66	3.9	1000	62
^{22}Na	1275	100	0.61	4.0	200	67

Table 10.23. Typical detection characteristics of a lung counter (4 HPGe semiconductor detectors as shown in Fig. 10.3.2.7) for homogeneous depositions of some selected actinides in the lungs (HPGe Anti-Compton counter of the Nuclear Research Centre Karlsruhe; subject counting time t_S = 3000 s; background counting time t_B = 30000 s)

Nuclide	Detected photon radiation		Counting efficiency η [%]	Background count rate N_B/t_B [cps]	Lower limit of detection [Bq]	
	Energy [keV]	Emission probability [%]			Required (Table 10.12)	Achieved
^{239}Pu	17.1(L_β)	2.3	0.017	0.0088	2	1500
^{241}Am	59.6	35.9	0.47	0.0090	0.2	3.6
^{235}U	186	57	0.24	0.0041	3	3.0

1) Calibration with LLNL chest phantom for 25 mm chest wall thickness and 50/50 muscle/adipose tissue composition

10.3.2.9 Measurement procedure

Subjects for direct measurements should be free of external surface contamination and in fresh clothing, often disposable paper garments. Accessories such as jewellery, watches and spectacles should be removed. Such precautions help to avoid false identifications of internal activity, and also prevent the transfer of contamination to the counting equipment. Individuals should, to the extent practicable, be in a defined counting position, to ensure reproducibility in serial measurements and to improve comparison with calibration results. In some cases the subject will need to remain stationary for periods up to an hour for satisfactory precision in the measurement. Some means of communication should be provided for subjects in enclosed shielding, particularly when extended counting periods are necessary.

For counting systems based on scintillation counting (NaI(Tl) crystals or phoswich detectors), background counts for the detector system should therefore be determined using an appropriate phantom, as similar as possible to the subject to be counted and placed in the defined counting position. For whole body counting, background counts determined using uncontaminated subjects matched with respect to gender, height and weight would improve results. Measurements of background in the counter should be made as close as possible in time to the measurement of the subject, ideally just before and just after. When using semiconductor detectors, background counting with matching phantoms is not necessary.

10.3.2.10 Quality assurance and control

Quality assurance (QA) for the measurement of internally deposited radionuclides includes all steps necessary to confirm the accuracy of the measurement and the validity of the dosimetrc interpretation. Guidance for quality assurance is provided by international institutions such as the International Standards Organization as well as by national authorities. The nature and extent of the QA programme should be consistent with the number of workers monitored, and the magnitude and likelihood of exposures expected in the workplaces to be covered by the monitoring programme.

All persons involved in the internal exposure assessment programme are responsible for its quality and therefore for implementing its QA programme and quality control (QC) procedures. Responsibility for the quality of a particular operation should be delegated to the person actually performing the operation. Such persons should be actively involved in the development of QC procedures, and trained in methods of detecting non-compliance.

A direct measurement facility should have a designated QA representative. This representative should monitor QC procedures, perform internal audits of the programme, and be responsible for training all personnel in QA, both in general terms and in the specific quality aspects of their individual work.

The fundamental requirements for a complete programme of QA include:

- compliance with general operational requirements stated in accepted written criteria
- a clearly documented in-house QA program
- periodic performance evaluations, including proficiency measurement tests
- documented procedures and quality assurance programme for services provided to customers

Quality control

Quality control in a measurement process is important to ensure that assessment of intakes is as reliable as possible. Evidence of the validity of such assessments may be required for legal and/or regulatory purposes.

Quality control programmes include the following activities:

- procedures and protocols for proper management of the internal dosimetry programme,
- detector system verification,
- routine verification of proper instrument performance,
- data recording and archiving,
- audits and accreditation,
- intercomparison [01Ram, 00Doe].

Procedures and protocols

The laboratory should prepare and maintain an operational manual that outlines responsibilities and provides requirements for data control, document control, maintenance/test, equipment calibration and checks, procedure, training, corrective action in the event of non-compliance, and traceability to standardizing bodies. The operations manual should include procedures to verify that the quality of the measurements meets the appropriate accuracy requirements. The quality control procedures should be carried out at appropriate intervals.

Performance checks

Performance checks of the system include energy calibration, energy resolution measurement and determination of the relative counting efficiency, generally using a point source.

National regulations may require that facilities concerned with measurement and internal dose assessment be accredited. Such accreditation programmes will have specifications for QA and QC to be implemented.

10.3.2.11 References for 10.3.2

27Blu Blumgart, H.I., Weiss, S.: J. Clin. Invest. **4** (1927) 389.
29Sch Schlundt, H., Barker, H.H., Flinn, F.B.: Am. J. Roentgenol. **21** (1929) 345.
31Sch Schlundt, H., Nerancy, J.T., Morris, J.P.: Am. J. Roentgenol. **26** (1931) 112.
37Eva Evans, R.: Am. J. Roentgenol. Radium Ther. **37** (1937) 368.
41Raj Rajewsky, B.: Strahlentherapie **69** (1941) 438.
51Sie Sievert, R.M.: Ark. Fys. **3** (1951) 337.
57And Anderson, E.C.: Br. J. Radiol., Suppl. **7** (1957) 27.
57Sie Sievert, R.M., Hultqvist, B.: Br. J. Radiol., Suppl. **7** (1957) 1.
58Bir Bird, P.M., Burch, P.R.J.: Phys. Med. Biol. **2** (1958) 217.
61Kie Kiefer, H., Maushart, R.: Kerntechnik **3** (1961) 228.
61Lan Langham, W.H., in: Radioactivity in Man. Thomas, G.C. (ed.), Springfield, IL: Charles C. Thomas, 1961, p. 311.
62Bur Burch, P.R.J., Hughes, D., Hnuma, T.A., Overton, T.R., Appleby, D.B., in: Proc. IAEA Symp. On Whole Body Counting, Vienna, Austria, 12-16 June 1961, Vienna: IAEA, 1962, p. 59.
63Alt Altshuler, B., Pasternack, B.: Health Phys. **9** (1963) 293.
64Kau Kaul, A., Schoeppe, W., Koch, K.M., Hierholzer, K.: Biophysik **2** (1964) 87.
64Raj Rajewsky, B., Kaul, A. and Heyder, J., In: Assessment of Radioactivity in Man **1,** Vienna: IAEA STI/PUB/84 (1964) 15.
68Cur Currie, L.A.: Anal. Chem. **40** (1968) 586.
68Lau Laurer, G.R.: The *in vivo* measurement of lung burdens of radionuclides emitting soft, penetrating radiations, available from: UMI, 300 N. Zeeb Rd. Ann Arbor, MI, USA, Order 6904570, 1968.
70IAE International Atomic Energy Agency. Directory of whole-body radioactive monitoring. STI/PUB/213, Vienna: IAEA, 1970, ISBN 02-0-112070-2.
72Par Parr, R. M., Dudley, R. A., Fedorov, G. A., In: Assessment of Radioactive Contamination in Man, Vienna: IAEA STI/PUB/290 (1972) 215.
75And Andrasi, A., Kotel, G.: Int. J. Appl. Radiat. Isot. **26** (1975) 451.
75ICR International Commission on Radiological Protection, ICRP Publication 23, Oxford and New York: Pergamon Press, 1975.
76Fal Falk, R.B., Tyree, W.H., Wood, C.B., Lagerquist, C.R.A., in: Advances in Radiation Protection Monitoring. Proceedings of a Symposium, Stockholm, Sweden, 26-30 June 1978, Vienna; IAEA, 1979, p. 445.
76Sch Schmitt, A., Fessler, H., in: Diagnosis and Treatment of Incorporated Radionuclides. Proceedings of a Symposium. STI/PUB/411, Vienna: IAEA, 1976, p. 285.
78New Newton, D., Fry, F.A., Taylor, B.T., Eagle, M.C., Sharma, R.C.: Health Phys. **35** (1978) 751.
79Gri Griffith, R.V., Dean, P.N., Anderson, A.L., Fisher, J.C., in: Advances in Radiation Protection Monitoring, Vienna: IAEA, 1979, p. 493.
80Tai Tait, W.H.: Radiation Detection, London: Butterworth & Co., 1980.
83ICR International Commission on Radiological Protection, ICRP Publication 38. Ann. ICRP 11-12, Oxford and New York: Pergamon Press, 1983.
83Too Toohey, R.E., Keane, A.T., Rundo, J.: Health Phys. **44**, Suppl. 1 (1983) 323.
85And Andrasi, A. Beleznay, E. and Urban, J. In: Assessment of Radioactive Contamination in Man, Vienna: IAEA STI/PUB/674 (1985) 165.
85New Newton, D., Wells, A. C., Mizushita, S., Toohey, R. E., Sha, J. Y., Jones, R., Jefferies, S. J., Palmer, H. E., Riekst, G. A., Anderson, A. L., Campbell, G. W., In: Assessment of Radioactive Contamination in Man, Vienna: IAEA STI/PUB/674 (1985) 183.
85Sch Shen, C., Wen, H., Zheng, W., Zhao, Y., Tang, M., Ye, C., Wu, D., In: Assessment of Radioactive Contamination in Man. Proc. Symp. Paris, France, 19-23 November 1984, Vienna: IAEA STI/PUB/674 (1985) 123.
85Sum Sumerling, T.J., McClure, D.R., Massey, D.K.: NRPB-R188, London: HMSO, 1985.
87ISO International Organization for Standardization, International Standard ISO9000, Geneva: ISO, 1987.

88ICR International Commission on Radiological Protection, ICRP Publication 54. Ann. ICRP 19 (1-3), Oxford and New York: Pergamon Press, 1988.
91Too Toohey, R.E.: Health Phys. **60**, Suppl. 1 (1991) 7.
92Del Delaney, C.F.G., Finch, E.C.: Radiation detectors, Oxford: Clarendon Press, 1992.
92Zik Zikovski, L., Kennedy, G.: Health Phys. **63** (1992) 449.
94And Andrasi, A., Henrichs, K., Bogner, L.: Report EUR 15395 EN, 1994.
94IAE International Atomic Energy Agency. TECDOC-746, Vienna: IAEA, 1994.
94ICR International Commission on Radiological Protection, ICRP Publication 68. Ann. ICRP 24(4), Oxford and New York: Pergamon Press, 1994.
94Skr Skrable, K. W., Chabot, G. E., French, C. S., LaBone, T. R.: Internal Radiation Dosimetry (RAABE, O.G., Ed.), Medical Physics Publishing, Madison, WI (1994) 431.
95Doe Doerfel, H.: Proc. Symposium on Radiation Protection in Neighboring Countries in Central Europe, Portoroz, 1995.
95Hub Hubbel, J.H., Seltzer, S.M.: National Institute of Standards and Technology, NISTIR 5632, 1995.
95Mal Mallett, M.W., Hickman, D.P., Knuchen, D.A., Poston, J.W.: Health Phys. **68** (6) (1995) 773.
96HPS Health Physics Society: Performance Criteria for Radiobioassay: American National Standards Institute HPS N13.30-1996, McLean, VA: Health Physics Society, 1996.
96IAE International Atomic Energy Agency.: Safety Series No. 114, Vienna: IAEA, 1996.
96Kra Kramer, G.H., Loesch, R.M., Olsen, P.C.: Proc. 1996 International Congress on Radiation Protection, Vienna,. **2** (1996) 409.
97ICR International Commission on Radiological Protection: ICRP Publication 78. Ann. ICRP 27(3/4), Oxford and New York: Pergamon Press, 1997.
98ISO International Organization for Standardization: International Standard ISO/WD 11929-8/ISO/TC85/SC2/WG5, Geneva: ISO, 1998.
99Kno Knoll, G.F.: Radiation Detection and Measurement, 3rd edn, New York: John Wiley & Sons, 1999.
99USD United States Department of Energy, DOE Standard DOE-STD-1112-98, 1999.
00And Andrasi, A.: Radiat. Prot. Dosim. **89** (3-4) (2000) 229.
00Doe Doerfel, H., Andrasi, A., Bailey, M.R., Birchall, A., Castellani, C.-M., Hurtgen, C., Jarvis, N., Johansson, L., LeGuen, B., Tarroni, G.: Forschungszentrum Karlsruhe GmbH, FZKA 6457, 2000.
00Lop López Ponte, M.A., Bravo, T.N.: Radiat. Prot. Dosim. **89** (3-4) (2000) 221.
01Ish Ishigure, N., Nakano, T., Enomoto. H.: Radiat. Prot. Dosim. **97** (3) (2001) 271.
01Ram Ramzaev, V., Ishikawa, T. Hill, P., Rahola, T., Kaidanovsky, G., Yonehara. H., Hille, R., Uchiyama, M.: Radiat. Prot. Dosim. **98** (2) (2002) 179.
02Kra Kramer, G.H., Hauck, B.M.: Radiat. Prot. Dosim. **102** (4) (2002) 323.
02Sin Singh, I.S., Suri, M.M.K., Vidhani, J.M., Garg, S.P., Sharma, R.C.: Radiat. Prot. Dosim. **102** (2) (2002) 145.
03Doe Doerfel, H., Andrasi, A., Bailey, M.R., Berkovski, V., Castellani, C.-M., Hurtgen, C., Jourdain, J.-R., LeGuen, B.: Radiat. Prot. Dosim. **105** (1-4) (2003) 645.
03Hun Hunt, J.G., de S. Santos, D., da Silva, F.C., Malatova, I., Foltanova, S., Dantas, B.M., Azaredo, A.: Radiat. Prot. Dosim. **105** (1-4) (2003) 549.
04BMU Bundesministerium für Umwelt, Naturschutz und Reaktorsicherheit: Richtlinie zur Ermittlung der Körperdosis bei innerer Strahlenexposition, Bundesanzeiger, to be published (2004).